Article

Competitive Arsenate and Phosphate Adsorption on Ferrihydrite as Described by the CD-MUSIC Model

Jon Petter Gustafsson* and Juan Antelo

Cite This: *ACS Earth Space Chem.* 2022, 6, 1397−1406
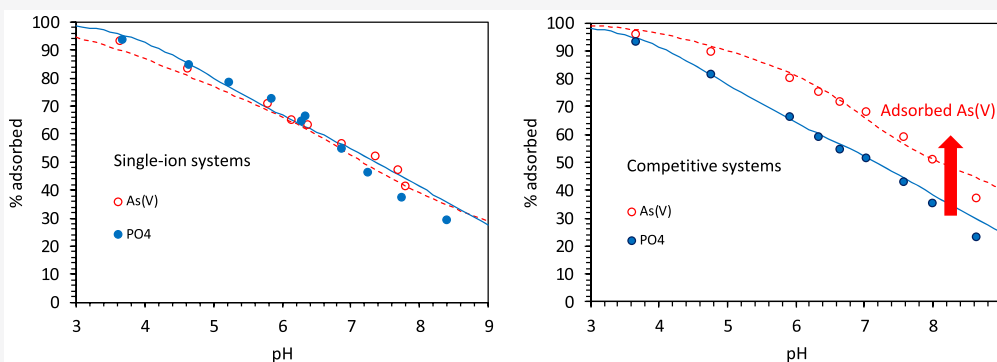
Read Online

ACCESS | 📊 Metrics & More | 📄 Article Recommendations | 🔘 Supporting Information

ABSTRACT: The solubility and bioavailability of arsenic in the environment are to a large extent governed by adsorption reactions with iron (hydr)oxides, the extent of which is affected by competitive interactions with other ions, for example, phosphate. Here, batch experiments were performed with ferrihydrite suspensions to determine the adsorption of arsenate $[As(V)]$ and phosphate (PO_4) at different $As(V)−PO_4$ ratios. A surface complexation model based on the Charge Distribution MUltisite Ion Complexation (CD-MUSIC) concept (the "Ferrihydrite CD-MUSIC model") was developed to describe these interactions in a way consistent with results from spectroscopic studies. For this purpose, several previously published data sets on $As(V)$ and PO_4 adsorption in ferrihydrite suspensions were reviewed, including a number of systems containing other major ions $(CO_3^{2−}$ and $Ca^{2+})$, and new surface complexation constants were derived. During model development, it was found that the inclusion of ternary complexes was not needed to describe the observed $Ca^{2+}−PO_4$ interactions. For both $As(V)$ and PO_4, the resulting model predicts the presence of corner-sharing bidentate complexes as well as monodentate complexes, with the latter being important particularly at low pH. The experimental results showed that $As(V)$ and PO_4 displayed similar adsorption patterns in the single-ion systems studied, which were conducted using a constant anion-to-Fe ratio of 0.2. Even so, $As(V)$ was preferentially adsorbed over PO_4 in competitive systems, particularly at low $As(V)$-to-PO_4 ratios when the K_d values for $As(V)$ were up to 2.1 times as high as those for PO_4. The model, which described these patterns very well, suggests that adsorbed $As(V)$ consists of a larger fraction of bidentate complexes than in the case of PO_4. This causes a flatter adsorption isotherm for $As(V)$, which leads to a stronger $As(V)$ adsorption as the $As(V)$-to-Fe ratio decreases, compared to that for PO_4.

KEYWORDS: *ferrihydrite, phosphate, arsenate, surface complexation modeling, CD-MUSIC, competitive binding*

■ INTRODUCTION

Iron (hydr)oxides have long been known for their high reactivity toward the environmentally important arsenate $[As(V)]$ and o-phosphate (PO_4) oxyanions.[1] Ferrihydrite, in particular, is an excellent adsorbent due in part to its very high specific surface area (SSA). In freshly prepared suspensions of 2-line ferrihydrite, the SSA can range from 500 to 800 $m^2\,g^{-1}$.[2] Other factors leading to the high reactivity toward $As(V)$ and PO_4 include a relatively high point of zero charge at around 8.1[3,4] and a high concentration of singly coordinated oxygens on the surface, resulting from a structure where relatively symmetrical iron(III) octahedra are sandwiched by asym-

metrical iron(III) octahedra and tetrahedra, where the two latter structures are depleted from the surface.[4−6]

In single-ion systems, that is, laboratory systems in which only one oxyanion is allowed to react with pure ferrihydrite or goethite, $As(V)$ and PO_4 are adsorbed to about the same extent across a wide range of pH values,[1,7] which can create the

impression that they are adsorbed in an identical fashion. However, in early works, it was observed that when both As(V) and PO_4 are present in the same suspensions, preferential adsorption of As(V) is observed.[1,8] Similar observations were made also more recently.[9−11] Despite the potential importance of this effect for correctly simulating, for example, levels of dissolved As(V) in the environment, so far there have been relatively few attempts in describing the preferential adsorption of As(V) on ferrihydrite in a quantitative manner that allows existing models, for example, surface complexation models (SCMs), to account for this.

Any differences in the binding strength of As(V) and PO_4 are probably related to differences in coordination at the surface. As concerns As(V), most results from extended X-ray absorption fine-structure (EXAFS) spectroscopy show As(V) to predominantly form corner-sharing (^2C) surface complexes on ferrihydrite and goethite, in which As(V) binds to two adjacent iron(III) octahedra.[11−16] This also agrees with molecular orbital (MO) calculations, applying density functional theory (DFT), which suggest that this coordination geometry is the most thermodynamically stable.[17] However, the presence of edge-sharing (^2E) complexes has also been reported in a few publications.[18,19] Moreover, monodentate complexes have been identified by attenuated total reflection (ATR)−Fourier transform infrared (FTIR) spectroscopy.[20−22] If present at relatively low concentrations, such complexes are difficult to identify with EXAFS spectroscopy due to the weak second-shell Fe···As interactions of such complexes. Still, in a few EXAFS studies, there was evidence for the presence of monodentate complexes.[12,13] For PO_4, the composition of surface complexes is more uncertain, in part due to the low molar mass of P, which makes EXAFS more difficult. However, Khare et al.[23] obtained X-ray absorption near-edge structure (XANES) evidence for a predominance of bidentate complexes on ferrihydrite at pH = 6. The presence of corner-sharing bidentate complexes on ferrihydrite between pH 3 and 8 has been shown by atomic pair distribution function analysis.[24] Arai and Sparks[25] used ATR−FTIR spectroscopy to conclude that nonprotonated bidentate complexes were likely dominant at pH > 7.5, whereas the data at pH < 7.5 could be described by different combinations of monodentate and bidentate complexes. On the other hand, Persson et al.[26] obtained FTIR spectra suggesting a predominance of monodentate complexes on goethite. Another study using ATR−FTIR suggested that PO_4 adsorption on iron (hydr)oxides can occur via a range of different mechanisms (monodentate/bidentate binding) that depend on the crystal faces present in the individual oxide preparation.[27]

Further insight into the likely mechanisms governing the interaction between As(V) and PO_4 can come from applying SCMs. Over the years, a number of models have been used for describing ion adsorption onto ferrihydrite. Examples include the generalized two-layer model and versions thereof,[3,28] the extended triple-layer model (ETLM),[29] and the Charge Distribution MUltisite Ion Complexation (CD-MUSIC) model.[30,31] As shown in many papers, these SCMs can describe the data of single-ion systems well. The challenge is to describe also competitive systems, with two or more interacting ions in the same system, in a consistent manner, which is commonly the case in the environment. It can be argued that if SCMs are to be used to infer anything about adsorption mechanisms, they should be shown to work not only for single-ion systems but also for various types of multicomponent systems.

Many attempts have been made to test SCMs in binary systems, with mixed results. One example is the work of Kanematsu et al.,[32] who used the ETLM to simulate As(V) adsorption to goethite in the presence of PO_4 or Ca^{2+}. Although As(V) was well described in single-ion systems, and also worked well to describe As(V) in binary systems with PO_4, the effect of Ca^{2+}, causing an enhanced As(V) adsorption, could not be correctly captured by the model. Furthermore, almost all SCMs, including the previous version of our own CD-MUSIC model for ferrihydrite,[33] fail when applying them to the binary PO_4−CO_3 systems of Mendez and Hiemstra.[34] Recently, Hiemstra and Zhao[31] moved forward with an updated Ferrihydrite CD-MUSIC model that divides the singly coordinated ≡FeOH sites into two groups, one that is able to form ^2C complexes and one that can form ^2E complexes, whereas both groups can form monodentate complexes. This model was used to investigate PO_4 adsorption as affected by the presence of Ca^{2+}, Mg^{2+}, and $CO_3^{2−}$.[34,35] It was concluded not only that a model in which PO_4 was bound as a mixture of monodentate and bidentate complexes worked well to describe these interactions but also that ternary Ca−PO_4−Fh and Mg−PO_4−Fh (Fh is for ferrihydrite) complexes needed to be accounted for in the modeling. As this model has shown to be able to handle competitive interactions in a better way than previous models, it serves as a starting point for the modeling exercise in the current paper.

Although the competition between As(V) and PO_4 on ferrihydrite has been studied previously,[8,9,36] these data were obtained only over a relatively limited range of conditions and were often incomplete, for example, no PO_4 data for single-ion systems were collected in the two latter studies, which makes it difficult to properly evaluate As(V)−PO_4 competition with SCMs. The current work supplies data for the competitive interactions of As(V) and PO_4 on ferrihydrite over a wider range of conditions by varying the As/P ratio in the system. The Ferrihydrite CD-MUSIC model is then optimized for single-ion systems of As(V), PO_4, Ca^{2+}, and $CO_3^{2−}$, considering also the model performance in binary systems. Model parameters were optimized in an iterative process where the goal was to arrive at a consistent model able to describe ion adsorption across a wide range of conditions. The resulting model was then applied to simulate the interactions in competitive systems consisting of As(V), PO_4, and ferrihydrite. The overall aim of this work was to assess the extent of preferential As(V) adsorption over PO_4 and to obtain clues on the mechanisms involved. As shown later, the model suggests that the observed fractionation effect is due to the higher proportion of monodentate complexes in the case of PO_4. Moreover, our model suggests that it is not necessary to account for ternary complexes to describe the interaction between PO_4 and Ca^{2+} on ferrihydrite.

■ MATERIALS AND METHODS

Ferrihydrite Synthesis. The procedure for the synthesis of ferrihydrite suspensions has been detailed earlier.[33,37] Briefly, 2-line ferrihydrite was synthesized with a method similar to the one described by Schwertmann and Cornell,[38] in which a solution containing 36 mM $Fe(NO_3)_3$ and 12 mM $NaNO_3$ was brought to pH 8.0 after dropwise addition of 4 M NaOH, after which the suspension was aged for 18 h. Before the start of the batch experiments, the suspension was brought back to pH 4.6

using 1 M HNO_3 and then shaken vigorously on a magnetic stirrer for at least 15 min to remove excess CO_2. Fe(III) oxide formed by this procedure has been confirmed to consist of 2-line ferrihydrite,[11] and the SSA has been estimated to be 611 $m^2\ g^{-1}$.[31]

Batch Experiments. All reacted suspensions contained a background electrolyte of 0.01 M $NaNO_3$. In one set of experiments carried out by Carin Sjöstedt at the Swedish University of Agricultural Sciences, As(V) adsorption as a function of pH was studied by mixing an amount of ferrihydrite stock suspension with $NaNO_3$ in a 40 mL polypropylene centrifuge bottle to which a certain volume of stock solution (18 mM Na_2HAsO_4) was added to produce the desired concentration (Table S3 and Figure S3f). Different additions of 0.01 M HNO_3 or 0.01 M NaOH were used to produce a range of pH values between pH 3 and 9. In another set of experiments conducted by the main author, the competition between As(V) and PO_4 was studied in a similar way using a fixed ferrihydrite concentration (as 1 mM Fe). Five different combinations of As(V) and/or PO_4 were used, that is, (i) 200 $\mu mol\ L^{-1}$ As(V); (ii) 200 $\mu mol\ L^{-1}$ PO_4; (iii) 100 $\mu mol\ L^{-1}$ As(V) + 100 $\mu mol\ L^{-1}$ PO_4; (iv) 160 $\mu mol\ L^{-1}$ As(V) + 40 $\mu mol\ L^{-1}$ PO_4; and (v) 40 $\mu mol\ L^{-1}$ As(V) + 160 $\mu mol\ L^{-1}$, using stock solutions of 6 mM Na_2HAsO_4 and 6 mM NaH_2PO_4. To ensure maximum consistency between the series, the whole set of experiments was carried out with the same ferrihydrite batch and at the same time (1−2 July 2021). In all experiments, the suspensions were shaken on an end-over-end shaker at 22 °C for 24 h prior to centrifugation and filtration using 0.2 μm single-use Acrodisc PF filters (Pall Corporation, Ann Arbor, MI, USA). The pH was measured on unfiltered samples using a Radiometer PHM93 pH meter equipped with a combination electrode (Radiometer Analytical SAS, Lyon, France). The filtered samples were acidified to 1% HNO_3 before determination of As and P with inductively coupled plasma−optical emission spectrometry using a Thermo iCAP 6300 instrument (Thermo Fisher Scientific, Waltham, MA, USA). No unexpected or unusually high safety hazards were encountered during these experiments.

Ferrihydrite CD-MUSIC Model. The version of the CD-MUSIC model used here employs the same division of sites between singly and triply coordinated groups as the model by Hiemstra and Zhao,[31] that is, with site densities of 5.8 and 1.4 sites nm^{-2}, respectively (Table 1). The singly coordinated sites

Table 1. Sites in the Ferrihydrite CD-MUSIC Model

site	site density (sites nm^{-2})
$\equiv FeOeH$	2.942
$\equiv FeOeH(h)$	0.058
$\equiv FeOcH$	2.742
$\equiv FeOcH(h)$	0.058
$\equiv Fe_3O$	1.4

are divided into two groups, one able to form edge-sharing and the other able to form corner-sharing bidentate complexes, here referred to as $\equiv FeOeH$ and $\equiv FeOcH$. These have site densities of 3.0 and 2.8 sites nm^{-2}, respectively. Moreover, within each group, there are subgroups of high-affinity sites, referred to as $\equiv FeOeH(h)$ and $\equiv FeOcH(h)$, which both have a site density of 0.058 sites nm^{-2}. The latter assignment differs from that by Mendez and Hiemstra,[35,39] who only considered $\equiv FeOcH(h)$ having a site density of 0.32 sites nm^{-2}. All singly

coordinated sites (i.e., both $\equiv FeOeH$ and $\equiv FeOcH$, the sum of which is simply referred to as $\equiv FeOH$) are able to bind monodentate complexes. The triply coordinated $\equiv Fe_3O$ sites do not form inner-sphere surface complexes in the model but may form outer-sphere complexes with an equal affinity to that of the $\equiv FeOH$ sites.

Furthermore, the model uses equations that relate the molar weight and the Stern layer capacitances $C_{1,r}$ and $C_{2,r}$ to the SSA, reflecting the nanoparticle dimensions of ferrihydrite assuming a spherical geometry[40] (see the Supporting Information). Hence, the model used in this paper simulates the acid−base characteristics of Fh in an identical manner as in the cited papers, and therefore, the same equilibrium constants for proton binding and ion-pair formation were used (see Table S1, Supporting Information).

Model Application. The Ferrihydrite CD-MUSIC model was optimized for As(V), PO_4, Ca^{2+}, and CO_3^{2-} using data from single-ion systems. For this purpose, the available literature was screened for published data that fulfilled the following criteria: (i) 2-line Fh should have been used in the experiments. If this was not confirmed in the study, the synthesis process should at least have been well described and consistent with the formation of 2-line Fh. (ii) The data should indicate an SSA of at least 500 $m^2\ g^{-1}$. Lower SSAs often result from drying/freeze-drying the Fh product, leading to aggregation. Because the aggregated Fh may disaggregate to an unknown extent during equilibration, this leads to difficulties with the data interpretation. (iii) An equilibration time of >2 h should be used as the observed adsorption may depend on this parameter.[3,41] Finally, (iv) only "adsorption edge" data were included, in which the adsorption was studied as a function of pH. Moreover, because the Fh synthesis conditions may vary, the SSA may vary slightly and can be treated as an adjustable parameter to fit PO_4 or As(V) adsorption data at high surface coverage.[40] In the current study, the same SSAs were used as those in the recent applications of the CD-MUSIC model for Fh, and some additional SSAs were adjusted from the default value of 611 $m^2\ g^{-1}$ to improve the fit at high surface coverage (for values cf. Tables S2−S5).

The selected data sets are described in the Supporting Information in Tables S2 (PO_4), S3 [As(V)], S4 (Ca^{2+}), and S5 (CO_3^{2-}). For PO_4, 18 adsorption edges from eight studies were included. All were studies from the Wageningen and Uppsala research groups, including data from two MSc theses,[42,43] which have been shown earlier.[33] For AsO_4, 30 adsorption edges from eight studies were processed during model fitting. However, one data point ("outlier") from the data set of Dixit and Hering[36] was excluded from optimization as it affected the optimized model to an unreasonable extent (Figure 2 and Table S3). For Ca^{2+} and CO_3^{2-}, fewer studies met the criteria; for Ca^{2+}, there were four studies with 25 adsorption edges; and for CO_3^{2-}, only two studies with 5 adsorption edges. The surface complexations constants were obtained by model fitting, which was carried out with the Visual MINTEQ 4.0-PEST coupling[44,45] using % adsorbed as the fitting variable and by maximizing the correlation coefficient R, which is a goodness-of-fit parameter reported by PEST.[45] The aqueous speciation was modeled using the standard thermodynamic database of Visual MINTEQ (Table S6).[44] The Davies equation was used for activity corrections, except for systems with ionic strengths ≥0.5 mol L^{-1}, for which specific ion-interaction theory (SIT) was used.[46] In the
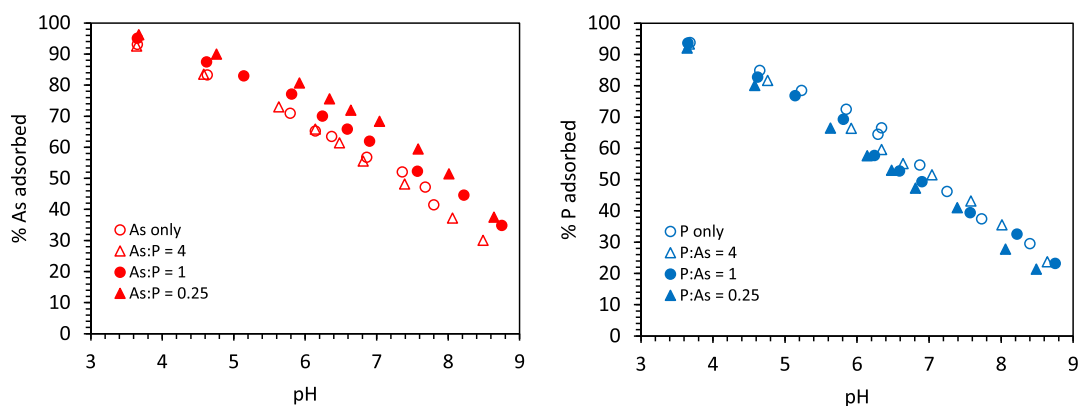
Figure 1. pH-dependent As(V) and PO_4 adsorption to ferrihydrite; $I = 0.01$ M $NaNO_3$, Fe = 1 mM, total P + As = 0.2 mM. Left: arsenate adsorption at different molar As/P ratios. Right: phosphate adsorption at different P/As molar ratios.

Table 2. Best-Fit Results for Surface Complexation Reactions in the Ferrihydrite CD-MUSIC Model

ion, model	no. of data points	surface complex	no. of H$^+$ in the reaction[a]	$(\Delta z_0, \Delta z_1)$[b]	log K[c]	same for high[d]	PEST R[e]
AsO_4^{3-}	317	$\equiv FeOAsO(OH)_2^{1/2-}$	3	(0.4, −0.4)	29.01 ± 0.14	y	0.990
		$\equiv FeOAsO_2OH^{11/2-}$	2	(0.35, −1.35)	25.30 ± 0.28	y	
		$(\equiv FeOc)_2AsOOH^-$	3	(0.58, −0.58)	33.06 ± 0.24	y	
		$(\equiv FeOc)_2AsO_2^{2-}$	2	(0.47, −1.47)	27.85 ± 0.04	y	
Ca^{2+}	215	$(\equiv FeOcH)_2Ca^+$	0	(0.6, 1.4)	3.46 ± 0.04	n	0.985
		$(\equiv FeOeH)_2Ca^+(h)$	0	(0.9, 1.1)	5.58 ± 0.10	n	
CO_3^{2-}	70	$(\equiv FeOc)_2CO^-$	2	(0.5, −0.5)	21.60 ± 0.06	y	0.961
		$\equiv FeOH_2^{1/2+}\cdots CO_3^{2-}$	1	(0.8, −1.8)	11.60	y	
		$\equiv Fe_3OH^{1/2+}\cdots CO_3^{2-}$	1	(0.8, −1.8)	11.60		
PO_4^{3-}	235	$\equiv FeOPO(OH)_2^{1/2-}$	3	(0.4, −0.4)	30.32 ± 0.08	y	0.995
		$\equiv FeOPO_2OH^{11/2-}$	2	(0.35, −1.35)	26.62 ± 0.08	y	
		$\equiv FeOPO_3^{21/2-}$	1	(0.25, −2.25)	18.00 ± 0.17	y	
		$(\equiv FeOc)_2POOH^-$	3	(0.65, −0.65)	33.19 ± 0.27	y	
		$(\equiv FeOc)_2PO_2^{2-}$	2	(0.46, −1.46)	27.93 ± 0.20	y	

[a]The stoichiometry of H$^+$ in the surface complexation reaction using $\equiv FeOH^{1/2-}$ as the surface component. [b]The change of charge in the 0 and 1 planes, respectively (CD factors). [c]The 95% confidence intervals according to PEST are shown. Values in italics: not fitted, constant, or tied during optimization (see text). [d]This column shows whether log K is the same for low- and high-affinity sites; y = yes and n = no. [e]The goodness-of-fit parameter as reported by PEST.[45]

modeling, we used the MO/DFT-calculated charge distribution (CD) factors of Hiemstra and co-workers as a starting point, but where relevant, these were adjusted for a better fit, while keeping to the guidelines defined by Rietra et al.[47]

The fitted model was applied also on selected data sets that did not meet the above criteria. This included the data sets of Antelo et al.,[7,48] which did not meet criterion (ii), that is, the SSA was too low. Still, these data sets were of considerable interest to include in the current study due to the data for the binary systems As(V)–Ca^{2+}–Fh and PO$_4$–Ca^{2+}–Fh. Acid–base titrations of Fh used in these studies can be successfully simulated using an SSA of 300 m^2 g^{-1} in combination with log K = 8.1 for the basic charging reaction[2] (Table S1). A problem, however, was that the use of this SSA provided model predictions that showed considerable underestimates of PO$_4$ adsorption at high pH and a sharper adsorption edge than was observed (Figure S1). We hypothesize that this occurred because of Fh disaggregation at high pH enabled by an increased negative surface charge, leading to a higher SSA in systems where PO$_4$ or As(V) was present. This is supported by simulations using the optimized Ferrihydrite CD-MUSIC model, which showed that the charge density of the diffuse layer changed from −0.002 C m^{-2} at pH 4 to −0.03 C m^{-2} at pH 8, using a 0.01 M NaNO$_3$ background and in the presence

of 0.6 mmol PO$_4$ L^{-1} in systems containing 11.4 mmol Fe L^{-1} as Fh. Hence, for the single-ion systems of Antelo et al.,[7,48] to which PO$_4$ or As(V) had been added, much improved model predictions of the adsorption isotherms were obtained when assuming that the SSA was variable. To derive such a model, the SSA was fitted for the PO$_4$ adsorption isotherms determined at pH 4.5, 7, 8, and 9.[48] Based on the resulting SSA values (250, 300, 350, and 400 m^2 g^{-1}, respectively), a second-order polynomial was derived to predict the variation of SSA with pH:

$$SSA\ (m^2\ g^{-1}) = 6.243 \times (pH)^2 - 50.52 \times pH + 350.6 \tag{1}$$

This equation was applied to all model predictions of Antelo et al.'s[7,48] data on PO$_4$ and As(V) adsorption in single-ion and binary systems as shown in this paper.

In the modeling, it was assumed that the formation of Fe(III) phosphate and arsenate minerals (e.g., strengite and scorodite) was insignificant. Although their solubility products were exceeded in some data sets, the results did not suggest any involvement of such a mineral phase. Recently, Wang et al. used P K-edge XANES spectroscopy to study PO$_4$ sorption mechanisms in similar batch experiments with ferrihydrite.[24] They observed Fe(III) phosphate precipitation in the mmol
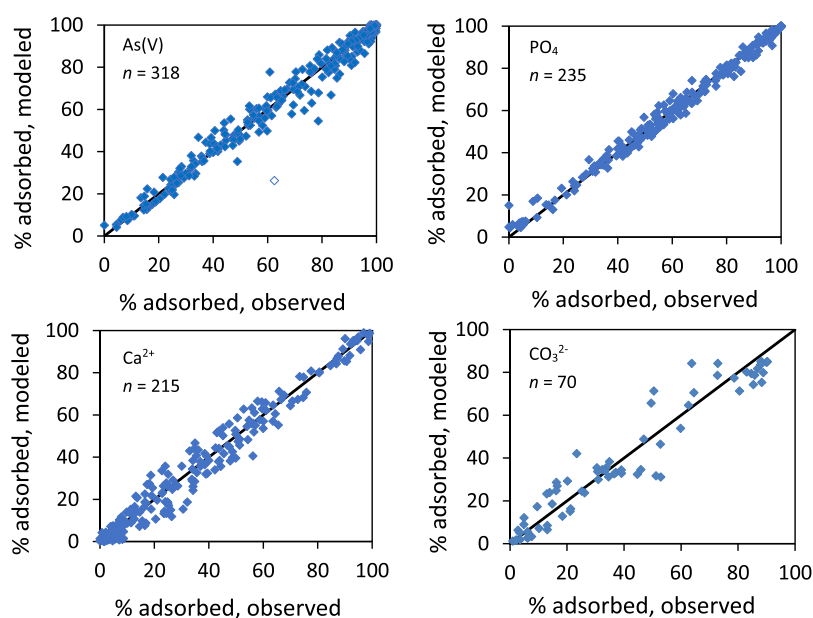
Figure 2. Modeled vs observed adsorption of As(V), PO$_4$, Ca^{2+}, and CO$_3^{2-}$ of the single-ion data sets (Table S1) using the surface complexation constants from Table 2. The empty data point among the As(V) data was excluded from optimization (cf. text).
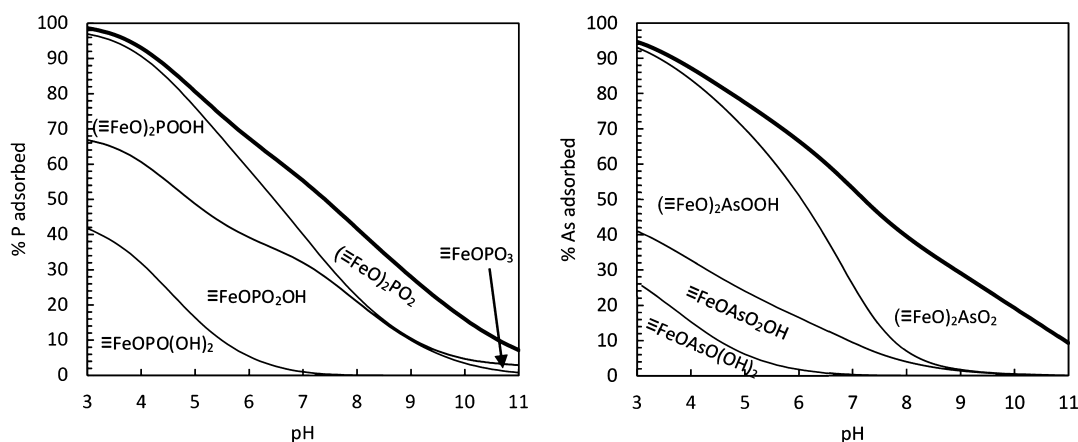

Figure 3. Modeled distribution of surface complexes as a function of pH for PO$_4$ (left) and for As(V) (right). Single-sorbate systems with PO$_4$ or As(V) = 200 μmol L^{-1}. Other conditions: I = 0.01 M NaNO$_3$, Fe = 1 mM, SSA = 611 m^2 g^{-1}, and T = 25 °C.

L^{-1} range (for PO$_4$) in combination with low pH values. All data treated in the current study were in the sub-mmol L^{-1} range except for a few data points of Hiemstra and Zhao,[31] for which the pH was very high (>10.5), making Fe(III) phosphate precipitation unlikely. For As(V), the situation is less clear. For some of the treated data sets, As(V) was in the mmol L^{-1} range (Figure S3), but since As(V) sorption could be described by a consistent set of adsorption parameters across all data sets, we consider that the formation of Fe(III) arsenate phases is unlikely/not significant.

Furthermore, for the binary systems of Ca^{2+}–PO$_4$ and Ca^{2+}–As(V) with Fh, the possible precipitation of amorphous Ca$_3$(PO$_4$)$_2$ × nH$_2$O (ACP) or Ca$_3$(AsO$_4$)$_2$ × nH$_2$O (ACA) phases was considered. For ACP, a log K_s of −27.94 was inferred from a study with filter materials used for wastewater treatment.[49] In the Fh systems analyzed in the current study, a higher solubility is likely due to the shorter equilibration time. We chose a log K_s of −27 and −27.5 for the data of Antelo et al.[7] and Mendez and Hiemstra,[35] respectively, judging from the shape of the adsorption edges at high pH. For similar reasons,

a log K_s of −20.5 was selected for ACA, which is slightly higher than the literature value of −21.14.[50]

RESULTS AND DISCUSSION

Batch Experiment Results. Although As(V) and PO$_4$ were adsorbed equally strongly across the studied pH range in single-ion systems, significant fractionation of As(V) over PO$_4$ was observed in binary systems, particularly at the low As/P ratios (Figure 1). In single-ion systems at pH 5.8, the K_d value of PO$_4$ (defined by the ratio of adsorbed to dissolved PO$_4$) was slightly higher than the K_d value of As(V), that is, 27,800 and 25,800 L kg^{-1}, respectively. However, in binary systems at an As/P ratio of 4 and under similar pH conditions (5.6), the K_d value was 1.3 times higher for As(V) than it was for PO$_4$. When the As/P ratios decreased further to 1 and 0.25, the K_d values of As(V) were 1.5 and 2.1 times higher, respectively (the pH values were 5.8 and 5.9). This supports earlier studies in which similar fractionation behavior was observed, that is, that As(V) is preferentially adsorbed.[8−10,36]
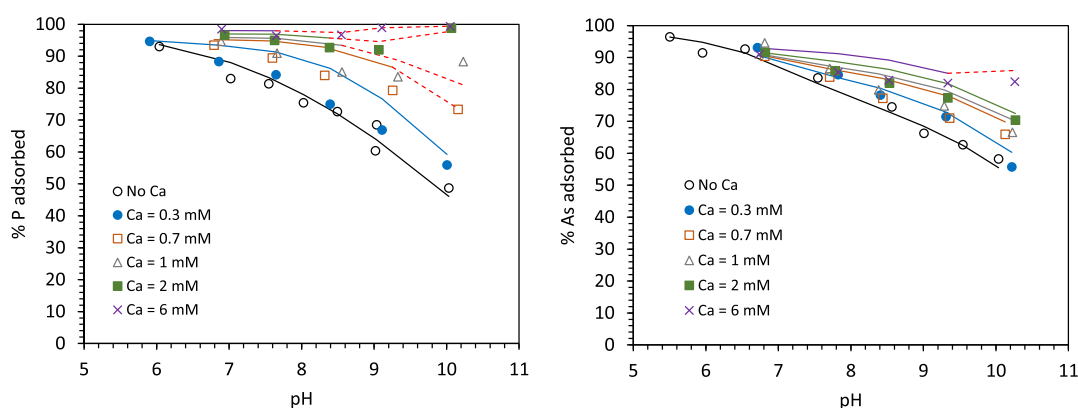
Figure 4. Effect of Ca^{2+} on the adsorption of PO_4 (left) and As(V) (right) as a function of pH. The symbols are observations of Antelo et al.,[7] and the lines are fits using the surface complexation constants of Table 2. The red dashed lines indicate modeled precipitation of $Ca_3(PO_4)_2 \times nH_2O$ or $Ca_3(AsO_4)_2 \times nH_2O$ using log $K_s = -27$ and -20.5, respectively (cf. text); $I = 0.1$ M KNO_3, Fe = 11.4 mM, initial PO_4 or As(V) = 0.6 mM. A variable SSA, calculated according to eq 1, was used.
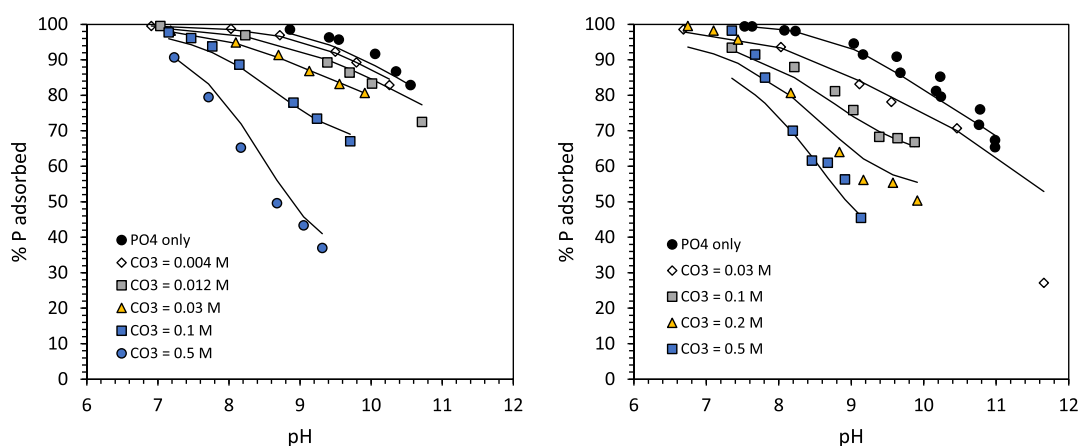

Figure 5. pH-dependent PO_4 adsorption as affected by CO_3^{2-} competition at $I = 0.5$ M. Symbols represent observations of Mendez and Hiemstra,[34] and lines are model fits using the surface complexation constants of Table 2. Left: $PO_4 = 0.251$ mM, Fe = 4.88 mM, SSA = 765 m^2 g^{-1}. Right: $PO_4 = 0.5$ mM, Fe = 7.2 mM, SSA = 672 m^2 g^{-1}.

Model Optimization: Phosphate. The studied data sets were highly consistent with regard to PO_4 binding, which resulted in excellent fits for the CD-MUSIC model (Table 2 and Figures 2 and S1). Consistent with Hiemstra and Zhao,[31] bidentate complexes were allowed on corner-sharing sites but not on the edge-sharing sites. No EXAFS data exist that corroborate this assignment, but given the small size of the PO_4 tetrahedron, it seems unlikely that it is able to form a stable edge-sharing bidentate complex with one iron(III) octahedron as this would lead to a substantial decrease of the O−Fe−O angle.[23] In all, five surface complexes were included in the model: the two bidentate complexes $(\equiv FeOc)_2POOH^-$ and $(\equiv FeOc)_2PO_2^{2-}$ and the three monodentate complexes $\equiv FeOPO(OH)_2^{1/2-}$, $\equiv FeOPO_2OH^{11/2-}$, and $\equiv FeOPO_3^{21/2-}$. The model is fairly similar to the one earlier proposed by Hiemstra and Zhao,[31] although the CD values of the monodentate complexes were adjusted slightly upward to improve the fit for the binary PO_4-CO_3 and $PO_4-As(V)$ systems. These CD values are, however, still within the range of "permitted" values.[47] Furthermore, a nonprotonated monodentate complex $\equiv FeOPO_3^{21/2-}$ was considered, which was found to be of some importance under high pH conditions (>10), although it was predicted only to play a minor role in PO_4 speciation under most circumstances (Figure 3). However, we found that the inclusion of the $\equiv FeOPO_3^{21/2-}$

complex improved the predictions of PO_4 binding in the binary PO_4-Ca^{2+} and $PO_4-CO_3^{2-}$ systems. As Figure 3 shows, the optimized model implies that a large part of the adsorbed PO_4 occurs as monodentate complexes, particularly at low pH when more than 50% of the adsorbed PO_4 is predicted to be monodentate. This percentage is predicted to increase in binary systems with Ca^{2+} and to decrease in systems with As(V) or CO_3^{2-} mainly because of the higher negative surface charge associated with the monodentate complexes. Also, as will be discussed below, the chosen PO_4 model was able to produce reasonably good predictions for the binary systems investigated, both for the $Ca^{2+}-PO_4$ systems (Figures 4 and S8) and for the $PO_4-CO_3^{2-}$ systems (Figures 5 and S10).

Model Optimization: Arsenate. Parameter values of the final selected model and its model fits for single-ion systems are shown in Table 2 and Figure S4, respectively, while the fit quality is shown in Figure 2. A number of different models, having different sets of parameter values, were able to provide reasonable fits to the single-ion arsenate adsorption data. In all these models, corner-sharing bidentate complexes accounted for the majority of the adsorbed As(V), in agreement with most EXAFS evidence, with monodentate complex(es) being of some additional significance at low pH. One possible modeling approach is to include only the two corner-sharing $(\equiv FeOc)_2AsOOH^-$ and $(\equiv FeOc)_2AsO_2^{2-}$ complexes, with
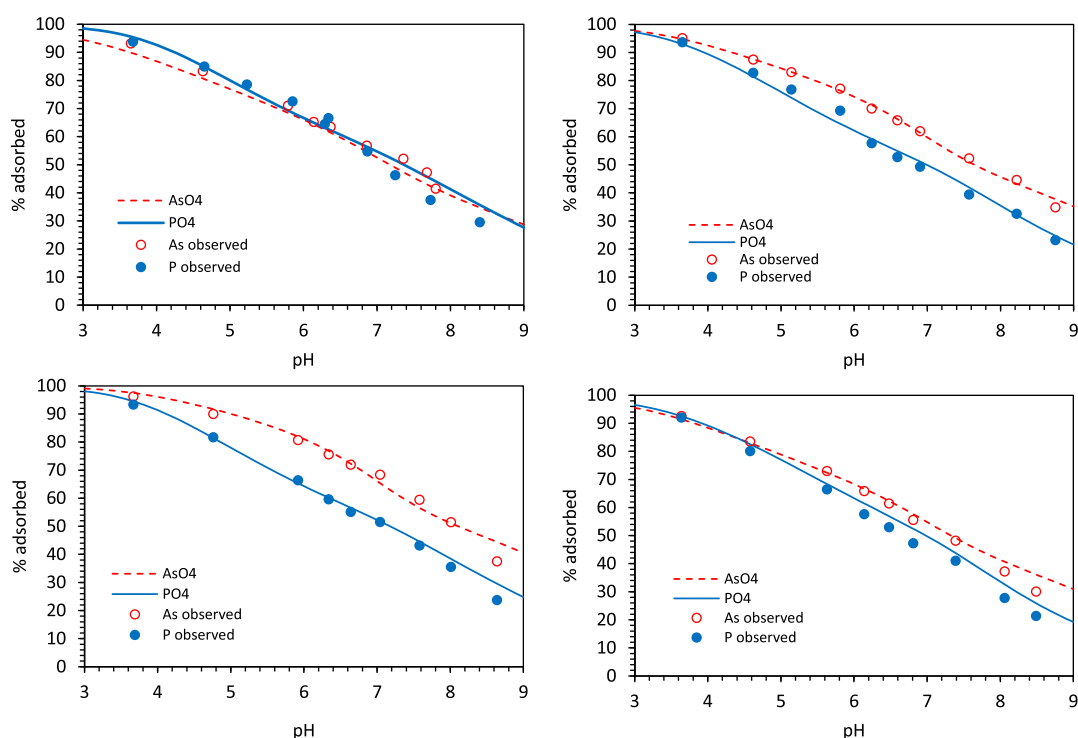
Figure 6. Competitive As(V) and PO_4 adsorption to ferrihydrite as a function of pH; $I = 0.01$ M $NaNO_3$, Fe = 1 mM, total P + As = 0.2 mM, SSA = 611 m^2 g^{-1}. Symbols represent observations, and model predictions are shown as lines. Upper left: single-sorbate systems of PO_4 = 0.2 mM or As(V) = 0.2 mM. Upper right: PO_4 = 0.1 mM and As(V) = 0.1 mM. Lower left: PO_4 = 0.16 mM and As(V) = 0.04 mM. Lower right: PO_4 = 0.04 mM and As(V) = 0.16 mM.

an additional diprotonated monodentate complex $\equiv FeOAsO-(OH)_2^{1/2-}$ which is of some importance at low pH. Such a model, however, was less successful in simulating the binary Ca−As(V) data provided by Antelo et al.[7] (Figure 4) as too little enhancement of As(V) adsorption was predicted in the presence of Ca^{2+} (data not shown). As a promoting effect of Ca^{2+} on As(V) has also been shown for goethite,[32,51] it seemed clear that an additional complex was needed. In agreement with Hiemstra and Zhao,[31] a second, monoprotonated, monodentate complex, $\equiv FeOAsO_2OH^{11/2-}$, was included. Although present at a relatively small concentration in single-ion systems (Figure 3), its significance increased in the presence of Ca^{2+}, leading to a promoting effect, although the fit was not perfect (Figure 4).

For the two data sets that were excluded from optimization due to an insufficient equilibration time,[52,53] the model overestimated As(V) adsorption (Figure S4), while the model-predicted As(V) sorption agreed well with the observations for the data set of Antelo et al.,[7] when using the model with a variable SSA. When using a fixed SSA, the model fit was much poorer, similar to what was found for PO_4 (data not shown).

Model Optimization: Calcium. No spectroscopic evidence exists concerning the adsorption mechanism of Ca^{2+} on iron(III) (hydr)oxides. Similar to previous model approaches, we assumed that Ca^{2+} forms bidentate complexes on Fh. In their CD-MUSIC model approach, Mendez and Hiemstra[39] recently assumed Ca^{2+} to form $(\equiv FeOcH)_2Ca^+$ complexes with relatively high CD values ($\Delta z_0 = 0.94$, $\Delta z_1 = 1.06$) involving also high-affinity sites with a higher log K (5.13, as compared to 2.64 for the low-affinity sites). The predominance of $(\equiv FeOcH)_2Ca^+$ is supported also by recent XANES evidence for goethite.[54] The model of Mendez and Hiemstra[38]

described their data well but was not able to describe $Ca^{2+}−PO_4$ binary systems without inclusion of a ternary Ca−PO$_4$−Fh complex. As there is no spectroscopic evidence for such a complex in the literature, we decided to investigate whether an alternative model could be formulated, without the need to consider ternary complexes. As a starting point, it was noted that the MO/DFT-calculated CD values of Mendez and Hiemstra[39] were based on the assumption of sixfold coordination of Ca^{2+} (i.e., CN = 6). The coordination number (CN) of Ca^{2+} in, for example, water molecules and minerals may, however, be variable, that is, in the range of 6−8;[54,55] a higher CN would lead to lower Δz_0 of the surface complex. We found that by using ($\Delta z_0 = 0.6$, $\Delta z_1 = 1.4$) for the low-affinity sites, while assuming that a small number of high-affinity sites could bind Ca^{2+} in a sixfold coordination ($\Delta z_0 = 0.9$, $\Delta z_1 = 1.1$), very good model fits were obtained for the single-ion systems including the isotherm obtained by Kinniburgh and Jackson[56] (Table 2 and Figures 2, S5, and S6). This six-coordinated Ca^{2+} was assumed to bind to the $\equiv FeOeH$ groups (i.e., as edge-sharing complexes), in agreement with the observation that six-coordinated Cd^{2+} is able to form such complexes on Fh.[57] With our model, reasonable model predictions were obtained for binary Ca−PO$_4$ systems *without* the need to include ternary complexes (Figure S9). In some of the binary Ca−PO$_4$ systems considered, the observed Ca−PO$_4$ interactions were very probably also affected by the precipitation of ACP, contributing to the Ca^{2+}-mediated increase in PO_4 retention (Figures 4 and S8).

Model Optimization: Carbonate. The coordination of carbonate on hydrated ferrihydrite was determined using ATR−FTIR spectroscopy[58,59] and was found to involve a corner-sharing bidentate complex $(\equiv FeOc)_2CO^-$ as well as an outer-sphere complex. The latter was assumed to be CO_3^{2-}

electrostatically attracted to $\equiv FeOH_2^{1/2+}$ and to $\equiv Fe_3OH^{1/2+}$ groups. In both available data sets (Table S5), the ($\equiv FeOc)_2CO^-$ complex was found to dominate. To fit these data, the CD values for this surface complex were adjusted from ($\Delta z_0 = 0.66$, $\Delta z_1 = -0.66$), as estimated from MO/DFT calculations,[34] to ($\Delta z_0 = 0.5$, $\Delta z_1 = -0.5$), which provided a much better fit to the adsorption edges of Zachara et al.,[60] which were not considered by Mendez and Hiemstra.[34] This difference could, to some extent, be ascribed to the uncertainty of using the correct template for MO/DFT modeling; by using a positively charged template consisting of two Fe octahedra, instead of an uncharged template, the Δz_0 value would be ~0.09 units lower.[34,61] However, also CD values of ($\Delta z_0 = 0.57$, $\Delta z_1 = -0.57$) produce clearly poorer fits to the data of Zachara et al.,[60] although it can be remarked that there is considerable scatter in this data set. In the absence of additional high-quality data that better constrain the CD values, we chose to use the lower Δz_0 value as it is based on experimental data, although it should be considered uncertain.

The surface complexation constant of the outer-sphere complex could not be constrained satisfactorily from the single-ion data, and instead, the constant was estimated to be log $K = 11.6$ based on the effect of CO_3 on PO_4 adsorption, cf. Table 2 and Figures 5 and S10. The model is slightly different from the one proposed by Mendez and Hiemstra,[34] who used a monodentate complex instead of an outer-sphere complex. These authors also used a second bidentate complex that involved an interaction with Na^+, which improved the model fit particularly at high pH. However, the model chosen in the current paper provided a reasonable description of the CO_3−PO_4 interaction, except for a few data points at very high pH. Furthermore, in some systems to which high CO_3 concentrations had been added, the model performed less satisfactorily at relatively low pH (Figures 5 and S10). In all these cases, the partial pressure of CO_2 was calculated to be >0.1 atm, which might have caused partial CO_2 degassing during the pH measurement and thus a higher pH. Because of the reasonably good model fit, it was decided not to include a third surface complex that would increase the degrees of freedom of the model.

Arsenate−Phosphate Interaction. With the PO_4 and As(V) surface complexation reactions constrained from the single-ion data sets, and from the other binary systems mentioned above, the Ferrihydrite CD-MUSIC model was able to provide a very good description of the observed fractionation between As(V) and PO_4 at the Fh−water interface, as observed in this study (Figure 6). The model was also able to predict As(V) and PO_4 competitive adsorption reasonably well for the dataset obtained by Jain and Loeppert,[9] while it underestimated As(V) adsorption as observed by Dixit and Hering (Figure S11).[34] However, the latter results are difficult to properly evaluate as no data were reported for PO_4 adsorption.

A key to understanding why the model predicts As(V) to be preferentially adsorbed in binary systems with both As(V) and PO_4 is provided by Figure 3. Although As(V) and PO_4 seem to form very similar surface complexes on Fh, the proportion of bidentate complexes is higher for As(V) than it is for PO_4. Because a bidentate complex occupies two $\equiv FeOH$ sites and a monodentate only one, it follows that site saturation is reached more quickly for As(V) than it is for PO_4, and consequently, the slope of the isotherm is smaller for As(V), see example in Figure S12. As a consequence, when decreasing the As(V)−

PO_4 ratio, As(V) adsorption will become relatively more efficient. In fact, the surface complexation constants of Table 2 actually imply a stronger As(V) adsorption than PO_4 adsorption at low anion to Fe ratios. A less important but contributing factor is that the formation of bidentate complexes affects the one-layer charge less than monodentate complexes at the same pH. Therefore, the adsorption of As(V) leads to less negative charge being accumulated in the one layer, at least if pH > 4. Under the conditions of the experiment, the Ferrihydrite CD-MUSIC model predicts the surface to have a net negative charge at pH > ~3.3 due to the adsorption of As(V) and PO_4. Hence, adsorbed As(V) can be accommodated somewhat more easily at pH > 4 in the competitive system. Similar reasons explain why (i) PO_4 is more sensitive to ionic strength variations, as was shown by Antelo et al.,[62] and (ii) PO_4 adsorption is enhanced more strongly by an adsorbing cation such as Ca^{2+}, as seen in Figure 4.

To the best of our knowledge, other published models are not currently able to predict the As(V)−PO_4 interactions observed in this study. For example, the generalized two-layer model of Dzombak and Morel[3] does not predict any preferential As(V) adsorption at all in binary systems. Our previous version of the CD-MUSIC model for ferrihydrite[33] does predict preferential As(V) adsorption but to a smaller extent than in the current study and does not adequately describe competitive interactions with Ca^{2+} and CO_3^{2-}. The CD-MUSIC model of Hiemstra and co-workers,[31,34,35,39,40] which served as an inspiration to the current model, does a better job in predicting competitive interactions with Ca^{2+} and CO_3^{2-} but predicts too strong As(V) adsorption at low pH under all conditions and thus incorrect fractionation behavior. Hence, the model version presented in the paper should offer an improved performance concerning As(V) and PO_4 adsorption in multicomponent, competitive systems under variable conditions (pH, ionic strength, and concentration levels).

■ CONCLUSIONS

In competitive systems with Fh, As(V) adsorbs more strongly than PO_4 when the two ions occur together, particularly at low As(V)−PO_4 ratios despite the fact that the adsorption of both appear to be equally strong when they occur in single-ion systems at high surface coverage. The observed fractionation is attributed mainly to the larger proportion of bidentate complexes for As(V), which leads to a flatter isotherm near site saturation; hence, As(V) adsorption is actually stronger than PO_4 at low anion-to-Fe ratios. The higher negative charge of monodentate complexes also contributes to the observed fractionation. Although the main trends are known since earlier, the data set provided in the current paper, as well as the improved model descriptions of As(V) and PO_4 binding in single-ion or multicomponent systems, will improve our ability to predict these effects qualitatively, which is of importance, for example, for correctly simulating As(V) solubility in contaminated materials.

Furthermore, when optimizing the CD-MUSIC model, it was shown that there is no need to consider a ternary $Ca-PO_4$ complex to properly describe the interactions between Ca^{2+} and PO_4 in systems with ferrihydrite, as was recently suggested.[35] By having a relatively low Δz_0 value for adsorbed Ca^{2+}, perhaps reflecting a high coordination number, or alternatively the presence of additional outer-sphere inter-

action mechanisms, the model adequately describes the promoting effect of Ca^{2+}. The same was true for the interaction between Ca^{2+} and As(V). Of course, this does not mean that such ternary complexes do not exist. Rather, these observations lead us to conclude that in order to better constrain the Ferrihydrite CD-MUSIC model and other similar models, it would be highly desirable to more precisely understand the surface complexation mechanisms of Ca^{2+}, alone and in systems with PO_4, with spectroscopy and other methods.

ASSOCIATED CONTENT

ⓈⒾ Supporting Information

The Supporting Information is available free of charge at https://pubs.acs.org/doi/10.1021/acsearthspace-chem.2c00081.

> Molar mass and Stern layer capacitances as a function of nanoparticle size; surface charging/ion-pair formation reactions used in the CD-MUSIC model; details on experimental conditions in single-ion systems; and additional figures of adsorption edges and isotherms in single-ion and competitive systems (PDF)
>
> Adsorption data (XLSX)

AUTHOR INFORMATION

Corresponding Author

Jon Petter Gustafsson − *Department of Soil and Environment, Swedish University of Agricultural Sciences, SE-750 07 Uppsala, Sweden;* ⓞ orcid.org/0000-0001-8771-7941; Email: jon-petter.gustafsson@slu.se

Author

Juan Antelo − *CRETUS, Department of Soil Science and Agricultural Chemistry, Universidade de Santiago de Compostela, 15782 Santiago de Compostela, Spain;* ⓞ orcid.org/0000-0002-9604-4635

Complete contact information is available at:
https://pubs.acs.org/10.1021/acsearthspacechem.2c00081

Notes

The authors declare no competing financial interest.

ACKNOWLEDGMENTS

REFERENCES

(1) Hingston, F. J.; Posner, A. M.; Quirk, J. P. Competitive adsorption of negatively charged ligands on oxide surfaces. *Discuss. Faraday Soc.* **1971**, *52*, 334−342.

(2) Mendez, J. C.; Hiemstra, T. Surface area of ferrihydrite consistently related to primary surface charge, ion pair formation, and specific ion adsorption. *Chem. Geol.* **2020**, *532*, 119304.

(3) Dzombak, D. A.; Morel, F. M. M. *Surface Complexation Modeling. Hydrous Ferric Oxide*; Wiley & Sons: New York, 1990.

(4) Hiemstra, T. Surface and mineral structure of ferrihydrite. *Geochim. Cosmochim. Acta* **2013**, *105*, 316−325.

(5) Michel, F. M.; Ehm, L.; Antao, S. M.; Lee, P. L.; Chupas, P. J.; Liu, G.; Strongin, D. R.; Schoonen, M. A. A.; Phillips, B. L.; Parise, J. B. The structure of ferrihydrite, a nanocrystalline material. *Science* **2007**, *316*, 1726−1729.

(6) Michel, F. M.; Barrón, V.; Torrent, J.; Morales, M. P.; Serna, C. J.; Boily, J.-F.; Liu, Q.; Ambrosini, A.; Cismasu, A. C.; Brown, G. E. Ordered ferrimagnetic form of ferrihydrite reveals links among structure, composition, and magnetism. *Proc. Natl. Acad. Sci. U.S.A.* **2010**, *107*, 2787−2792.

(7) Antelo, J.; Arce, F.; Fiol, S. Arsenate and phosphate adsorption on ferrihydrite nanoparticles. Synergetic interaction with calcium ions. *Chem. Geol.* **2015**, *410*, 53−62.

(8) Ryden, J. C.; Syers, J. K.; Tillman, R. W. Inorganic anion sorption and interactions with phosphate sorption by hydrous ferric oxide gel. *J. Soil Sci.* **1987**, *38*, 211−217.

(9) Jain, A.; Loeppert, R. H. Effect of Competing Anions on the Adsorption of Arsenate and Arsenite by Ferrihydrite. *J. Environ. Qual.* **2000**, *29*, 1422−1430.

(10) Carabante, I.; Grahn, M.; Holmgren, A.; Hedlund, J. In situ ATR-FTIR studies on the competitive adsorption of arsenate and phosphate on ferrihydrite. *J. Colloid Interface Sci.* **2010**, *351*, 523−531.

(11) Tiberg, C.; Sjöstedt, C.; Eriksson, A. K.; Klysubun, W.; Gustafsson, J. P. Phosphate competition with arsenate on poorly crystalline iron and aluminum (hydr)oxide mixtures. *Chemosphere* **2020**, *255*, 126937.

(12) Waychunas, G. A.; Rea, B. A.; Fuller, C. C.; Davis, J. A. Surface chemistry of ferrihydrite: Part 1. EXAFS studies of the geometry of coprecipitated and adsorbed arsenate. *Geochim. Cosmochim. Acta* **1993**, *57*, 2251−2269.

(13) Waychunas, G. A.; Davis, J. A.; Fuller, C. C. Geometry of sorbed arsenate on ferrihydrite and crystalline FeOOH: re-evaluation of EXAFS results and topological factors in predicting sorbate geometry, and evidence for monodentate complexes. *Geochim. Cosmochim. Acta* **1995**, *59*, 3655−3661.

(14) Farquhar, M. L.; Charnock, J. M.; Livens, F. R.; Vaughan, D. J. Mechanisms of arsenic uptake from aqueous solution by interaction with goethite, lepidocrocite, mackinawite, and pyrite: an X-ray absorption spectroscopy study. *Environ. Sci. Technol.* **2002**, *36*, 1757−1762.

(15) Voegelin, A.; Weber, F.-A.; Kretzschmar, R. Distribution and speciation of arsenic around roots in a contaminated riparian floodplain soil: micro-XRF element mapping and EXAFS spectroscopy. *Geochim. Cosmochim. Acta* **2007**, *71*, 5804−5820.

(16) Tiberg, C.; Kumpiene, J.; Gustafsson, J. P.; Marsz, A.; Persson, I.; Mench, M.; Kleja, D. B. Immobilization of Cu and As in two contaminated soils with zero-valent iron—Long-term performance and mechanisms. *Appl. Geochem.* **2016**, *67*, 144−152.

(17) Sherman, D. M.; Randall, S. R. Surface complexation of arsenic(V) to iron(III) (hydr)oxides: structural mechanism from ab initio molecular geometries and EXAFS spectroscopy. *Geochim. Cosmochim. Acta* **2003**, *67*, 4223−4230.

(18) Fendorf, S.; Eick, M. J.; Grossl, P.; Sparks, D. L. Arsenate and chromate retention mechanisms on goethite. 1. Surface structure. *Environ. Sci. Technol.* **1997**, *31*, 315−320.

(19) Neupane, G.; Donahoe, R. J.; Arai, Y. Kinetics of competitive adsorption/desorption of arsenate and phosphate at the ferrihydrite-water interface. *Chem. Geol.* **2014**, *368*, 31−38.

(20) Guan, X.-H.; Wang, J.; Chusuei, C. C. Removal of arsenic from water using granular ferric hydroxide: macroscopic and microscopic studies. *J. Hazard. Mater.* **2008**, *156*, 178−185.

(21) Loring, J. S.; Sandström, M. H.; Norén, K.; Persson, P. Rethinking arsenate coordination at the surface of goethite. *Chem.—Eur. J.* **2009**, *15*, 5063−5072.

(22) Li, X.; Yan, L.; Zhong, W.; Kersten, M.; Jing, C. Competitive arsenate and phosphate adsorption on α-FeOOH, LaOOH, and nano-TiO$_2$: two-dimensional correlation spectroscopy study. *J. Hazard. Mater.* **2021**, *414*, 125512.

(23) Khare, N.; Martin, J. D.; Hesterberg, D. Phosphate bonding configuration on ferrihydrite based on molecular orbital calculations and XANES fingerprinting. *Geochim. Cosmochim. Acta* **2007**, *71*, 4405−4415.

(24) Wang, X.; Hu, Y.; Tang, Y.; Yang, P.; Feng, X.; Xu, W.; Zhu, M. Phosphate and phytate adsorption and precipitation on ferrihydrite surfaces. *Environ. Sci.: Nano* **2017**, *4*, 2193−2204.

(25) Arai, Y.; Sparks, D. L. ATR-FTIR spectroscopic investigation on phosphate adsorption mechanisms at the ferrihydrite-water interface. *J. Colloid Interface Sci.* **2001**, *241*, 317−326.

(26) Persson, P.; Nilsson, N.; Sjöberg, S. Structure and bonding of orthophosphate ions at the iron oxide-aqueous interface. *J. Colloid Interface Sci.* **1996**, *177*, 263−275.

(27) Kubicki, J. D.; Paul, K. W.; Kabalan, L.; Zhu, Q.; Mrozik, M. K.; Aryanpour, M.; Pierre-Louis, A.-M.; Strongin, D. R. ATR-FTIR and Density Functional Theory Study of the Structures, Energetics, and Vibrational Spectra of Phosphate Adsorbed onto Goethite. *Langmuir* **2012**, *28*, 14573−14587.

(28) Nomaan, S. M.; Stokes, S. N.; Han, J.; Katz, L. E. Application of spectroscopic evidence to diffuse layer model (DLM) parameter estimation for cation adsorption onto ferrihydrite in single- and bi-solute systems. *Chem. Geol.* **2021**, *573*, 120199.

(29) Fukushi, K.; Okuyama, A.; Takeda, N.; Kosugi, S. Parameter-ization of adsorption onto minerals by Extended Triple Layer Model. *Appl. Geochem.* **2021**, *134*, 105087.

(30) Hiemstra, T.; van Riemsdijk, W. H. A surface structural approach to ion adsorption: the charge distribution (CD) model. *J. Colloid Interface Sci.* **1996**, *179*, 488−508.

(31) Hiemstra, T.; Zhao, Z. Reactivity of ferrihydrite and ferritin in relation to surface structure, size, and nanoparticle formation studied for phosphate and arsenate. *Environ. Sci.: Nano* **2016**, *3*, 1265−1279.

(32) Kanematsu, M.; Young, T. M.; Fukushi, K.; Green, P. G.; Darby, J. L. Arsenic(III, V) adsorption on a goethite-based adsorbent in the presence of major co-existing ions: Modeling competitive adsorption consistent with spectroscopic and molecular evidence. *Geochim. Cosmochim. Acta* **2013**, *106*, 404−428.

(33) Tiberg, C.; Sjöstedt, C.; Persson, I.; Gustafsson, J. P. Phosphate effects on copper(II) and lead(II) sorption to ferrihydrite. *Geochim. Cosmochim. Acta* **2013**, *120*, 140−157.

(34) Mendez, J. C.; Hiemstra, T. Carbonate adsorption to ferrihydrite: competitive interaction with phosphate for use in soil systems. *ACS Earth Space Chem.* **2019**, *3*, 129−141.

(35) Mendez, J. C.; Hiemstra, T. Ternary complex formation of phosphate with Ca and Mg ions binding to ferrihydrite: experiments and mechanisms. *ACS Earth Space Chem.* **2020**, *4*, 545−557.

(36) Dixit, S.; Hering, J. G. Comparison of arsenic(V) and arsenic(III) sorption onto iron oxide minerals: implications for arsenic mobility. *Environ. Sci. Technol.* **2003**, *37*, 4182−4189.

(37) Gustafsson, J. P. Modelling molybdate and tungstate adsorption to ferrihydrite. *Chem. Geol.* **2003**, *200*, 105−115.

(38) Schwertmann, U.; Cornell, R. L. *Iron Oxides in the Laboratory. Preparation and Characterization*; Wiley: Weinheim, 2000.

(39) Mendez, J. C.; Hiemstra, T. High and low affinity sites of ferrihydrite for metal ion adsorption: Data and modeling of the alkaline-earth ions Be, Mg, Ca, Sr, Ba, and Ra. *Geochim. Cosmochim. Acta* **2020**, *286*, 289−305.

(40) Hiemstra, T. Ferrihydrite interaction with silicate and competing oxyanions: Geometry and Hydrogen bonding of surface species. *Geochim. Cosmochim. Acta* **2018**, *238*, 453−476.

(41) Swedlund, P. J.; Holtkamp, H.; Song, Y.; Daughney, C. J. Arsenate-ferrihydrite systems from minutes to months: a macroscopic and IR spectroscopic study of an elusive equilibrium. *Environ. Sci. Technol.* **2014**, *48*, 2759−2765.

(42) Edkymish, A. Lead binding onto iron oxides (ferrihydrite) as influenced by aluminium and phosphorus. MSc Thesis LWR-EX-09-15, KTH Royal Institute of Technology, Stockholm, Sweden, 2009.

(43) Bertholds, C. Antimony, cobalt, and silver solubility in soil: an experimental and modelling study. MSc Thesis, Department of Soil Sciences, Swedish University of Agricultural Sciences, Uppsala, Sweden, 2009.

(44) Gustafsson, J. P. *Visual MINTEQ*, version 4.0 beta; SLU: Sweden, 2022. Web: https://vminteq.com/ (accessed April 25, 2022).

(45) Doherty, J. *PEST, Model-Independent Parameter Estimation, User Manual*, 5th ed.; Watermark Numerical Computing, 2010.

(46) Grenthe, I.; Plyasunov, A. V.; Spahiu, K.; Grenthe, I. Estimation of medium effects on thermodynamic data. In *Modelling in Aquatic Chemistry*; Puigdomenech, I., Ed.; Nuclear Energy Agency, OECD: Paris, 1997; pp 325−426.

(47) Rietra, R. P. J. J.; Hiemstra, T.; van Riemsdijk, W. H. The relationship between molecular structure and ion adsorption on variable charge minerals. *Geochim. Cosmochim. Acta* **1999**, *63*, 3009−3015.

(48) Antelo, J.; Fiol, S.; Pérez, C.; Mariño, S.; Arce, F.; Gondar, D.; López, R. Analysis of phosphate adsorption onto ferrihydrite using the CD-MUSIC model. *J. Colloid Interface Sci.* **2010**, *347*, 112−119.

(49) Gustafsson, J. P.; Renman, A.; Renman, G.; Poll, K. Phosphate removal by mineral-based sorbents used in filters for small-scale wastewater treatment. *Water Res.* **2008**, *42*, 189−197.

(50) Nordstrom, D. K.; Majzlan, J.; Königsberger, E. Thermody-namic Properties for Arsenic Minerals and Aqueous Species. *Rev. Mineral. Geochem.* **2014**, *79*, 217−255.

(51) Deng, Y.; Li, Y.; Li, X.; Sun, Y.; Ma, J.; Lei, M.; Weng, L. Influence of calcium and phosphate on pH dependency of arsenite and arsenate adsorption to goethite. *Chemosphere* **2018**, *199*, 617−624.

(52) Hsia, T.-H.; Lo, S.-L.; Lin, C.-F.; Lee, D.-Y. Characterization of arsenate adsorption on hydrous iron oxide using chemical and physical methods. *Colloids Surf., A* **1994**, *85*, 1−7.

(53) Wilkie, J. A.; Hering, J. G. Adsorption of arsenic onto hydrous ferric oxide: effects of adsorbate/adsorbent ratios and co-occurring solutes. *Colloids Surf., A* **1996**, *107*, 97−110.

(54) Jia, Y.; Zheng, Y.; Lin, J.; Zhang, G.; Ma, X.; Wang, X.; Wang, S. Surface sorption site and complexation structure of Ca^{2+} at the goethite-water interface: a molecular dynamics simulation and quantitative XANES analysis. *Bull. Environ. Contam. Toxicol.* **2019**, *103*, 64−68.

(55) Jalilehvand, F.; Spångberg, D.; Lindqvist-Reis, P.; Hermansson, K.; Persson, I.; Sandström, M. Hydration of the calcium ion. An EXAFS, large-angle X-ray scattering, and molecular dynamics simulation study. *J. Am. Chem. Soc.* **2001**, *123*, 431−441.

(56) Kinniburgh, D. G.; Jackson, M. L. Concentration and pH dependence of calcium and zinc adsorption by iron hydrous oxide gel. *Soil Sci. Soc. Am. J.* **1982**, *46*, 56−61.

(57) Tiberg, C.; Gustafsson, J. P. Phosphate effects on cadmium(II) sorption to ferrihydrite. *J. Colloid Interface Sci.* **2016**, *471*, 103−111.

(58) Hausner, D. B.; Bhandari, N.; Pierre-Louis, A.-M.; Kubicki, J. D.; Strongin, D. R. Ferrihydrite reactivity toward carbon dioxide. *J. Colloid Interface Sci.* **2009**, *337*, 492−500.

(59) Baltrusaitis, J.; Schuttlefield, J.; Zeitler, E.; Grassian, V. H. Carbon dioxide adsorption on oxide nanoparticle surfaces. *Chem. Eng. J.* **2011**, *170*, 471−481.

(60) Zachara, J. M.; Girvin, D. C.; Schmidt, R. L.; Resch, C. T. Chromate adsorption on amorphous iron oxyhydroxide in the presence of major groundwater ions. *Environ. Sci. Technol.* **1987**, *21*, 589−594.

(61) Rahnemaie, R.; Hiemstra, T.; van Riemsdijk, W. H. Carbonate adsorption on goethite in competition with phosphate. *J. Colloid Interface Sci.* **2007**, *315*, 415−425.

(62) Antelo, J.; Avena, M.; Fiol, S.; López, R.; Arce, F. Effects of pH and ionic strength on the adsorption of phosphate and arsenate at the goethite-water interface. *J. Colloid Interface Sci.* **2005**, *285*, 476−486.